International Journal of Advanced Science and Technology
Vol.71 (2014), pp.59-66
http://dx.doi.org/10.14257/ijast.2014.71.06

A Comparative Study on SiGe HBTs and Si BJTs in Nanoscale

P. Behera and S. K. Mohapatra*

Department of Electronics & Telecom Engineering,
Ajay Binay Institute of Technology (ABIT), Cuttack, 753014, Odisha, India.
p_behera_06@yahoo.co.in, s.k.mohapatra@ieee.org

Abstract

In this paper, a comparative study is done on performance of strained SiGe Heterojunction Bipolar Transistors (HBTs) with 100nm base width of conventional transistor. The device parameters like energy band gap variation, electron current density, electron drift velocity, electron and hole mobility are discussed. Here the current gain of strained SiGe layers was observed to increase by seven times as compared to bulk Si, because of the improvement in mobility in the trapezoid-base $Si_{0.88}Ge_{0.12}$ *HBT. The strained SiGe HBT had 0.07 v lower turn on voltage than BJTs. The DC current gain of SiGe HBT can be improved further, by increasing Ge mole fraction. The simulation and parameter extraction have been done through the device simulator atlas module of SILVACO software.*

Keywords: *strained silicon-germanium HBTs, different Ge profile, analog performance, voltage gain*

1. Introduction

In recent years, strained silicon germanium has been the focus of research for better performance of heterojunction bipolar transistors (HBTs). SiGe HBTs provide many advantages over the conventional Si homojunction bipolar transistors (Si-BJTs).The SiGe-HBTs offer vertical scaling with low base resistance for high speed performance, very high current gain and lower turn on voltage for analogue design. As a result, Strain silicon germanium is the most suitable material for analog, digital and mixed signal RF application [1].

During the last two decade there has been a rapid progress in SiGe based devices such as heterojunction bipolar transistors (SiGe-HBTs) and Field effect transistors (HFETs) [2,3]. Some of very promising results on SiGe-HBTs have been reported [4]. So strained SiGe is one of new technologies that enables a fairly dramatic increase in performance with a relatively change in germanium profile in starting materials [5]. A comparison of device performance is given in Table-1, it is seen that the SiGe-HBTs provide equal or better performance for low noise amplifier applications and IBMs SiGe-BiCMOS technologies allow for high levels of integration with a cost structure similar to standard silicon BiCMOS process [6]. When used for wireless applications in which the power supply is a battery, the SiGe process delivers high performance HBTs at almost 50% less prime power and much lower cost than GaAs [7].In this paper, we discuss the choice of Technology for analogue application. Attention the same geometry and doping profile. The DC performance of Si/SiGe HBTs has been simulated using a 2D DDT solver and current is drawn to the comparison of SiGe HBTs and Si BJTs devices. The devices examined have gain roll off SiGe HBT with different Ge percentage has been extracted using ATLAS simulator [19].

ISSN: 2005-4238 IJAST
Copyright ⓒ 2014 SERSC

Table 1. Technology Comparison

Parameters	Si BJT	SiGe HBT	GaAs HBT	GaAs HEMT
Pdc(mW)	40	16.2	29.1	20
Gain(dB)	17	12.5	29.1	20
NF(dB)	1.5	1.3	1.6	0.6
Linearity	4	19.5	11	10
Efficiency	High	High	Low	Low

2. Physical Modelling

The physical models involved in the simulation of Si BJTs and $S_{1-x}Ge_x$ HBTs are characterized by a set of fundamental equations which link the electrostatic potential and carrier densities within some predefined simulation domain. These equations are derived from Maxwell's laws and consist of Poisson's equation and the continuity equations for electrons and holes [8]. Poisson's equation relates variation in electrostatic potential to the space charge density and is given by [8].

$$\nabla.(\varepsilon\nabla \aleph) = -q\left(p - n + N_D^+ - N_A^-\right)\rho_s \tag{1}$$

Where $\aleph$ is the electrostatic potential, ε is the local dielectric permittivity, q is the charge of an electron, p and n are the hole and electron concentrations, and N_D^+ and N_D^- are the ionized donor and acceptor impurity concentrations. The continuity equations which describe the way that electron and hole carrier densities evolve as a result of transport processes, generation and recombination processes are given by,

$$\frac{\partial n}{\partial t} = \frac{1}{q}\nabla.\overrightarrow{Jn} + (M - N) \tag{2}$$

$$\frac{\partial p}{\partial t} = \frac{1}{q}\nabla.\overrightarrow{Jp} + (M - N) \tag{3}$$

Where *Jn* and *Jp* are the electron and hole current densities, M and N are the generation and the recombination rates. The current density equations are usually obtained by applying approximations and simplifications to the Boltzmann transport equations. In the drift-diffusion model, the current densities are expressed as [8].

$$\overrightarrow{Jn} = q\mu_n \vec{E}n + qD_n\nabla n \tag{4}$$

$$\overrightarrow{Jp} = q\mu_p \vec{E}p + qD_p\nabla p \tag{5}$$

Where μ_n and μ_p are the electron and hole mobility, and $Dn=kT_L/q\ \mu_n$ and $Dp=kT_L/q\ \mu_p$ are the electron and hole diffusion Constants. Drift-diffusion model for SiGe-HBTs, is based on the bipolar transistor modeling, and has been used in simulation. The model equations account for valence band discontinuity, heavy doping effects and high collector current effects. The additional build-in field due to the Ge concentration gradient is also taken into account.

Simulation has been carried out for generating Gummel plots and for studying enhancement of collector currents and their dependence on temperature. The transistor

Copyright ⓒ 2014 SERSC

is connected in common- emitter configuration with collector-emitter bias of 2V.The electron and hole life times in the SiGe layer are taken to be 10% of the values computed for pure silicon. The energy band gap values in the SiGe layer are computed using the model parameter [9]. The other parameters, such as dielectric constants, intrinsic carrier concentration life time etc. is also taken into account. Collector velocity overshoot will not significantly contribute to the reduction of total transit time [10]. In addition to these capabilities it uses into the high-frequency performance of RF/mixed signal application.

3. Material Parameters

The incorporation of germanium significantly changes the properties of the base-collector junctions in a Si/SiGe HBT. Addition of germanium reduces the band gap of Si leading to the narrow band gap SiGe base of the HBT. The lattice constant of SiGe alloy differs considerably from that of Si. Hence in the incorporation of Ge, various semiconductors differ in their fundamental properties such as band gap, carrier mobility, effective electron and hole masses, *etc*. In addition, interfaces between different materials must cause strain in the SiGe HBT which is compressive in plane, modifying the energy band structure and density of states in the conduction and valence bands [11].In Figure 1(a). Reviews about the conduction band edge of unstrained Si and strained SiGe alloys. The constant energy surface of the strained SiGe is grown on <001> Si substrate. So that the change in size of each valley in a constant energy surface indicates a shift up (smaller) or down (larger) in energy.

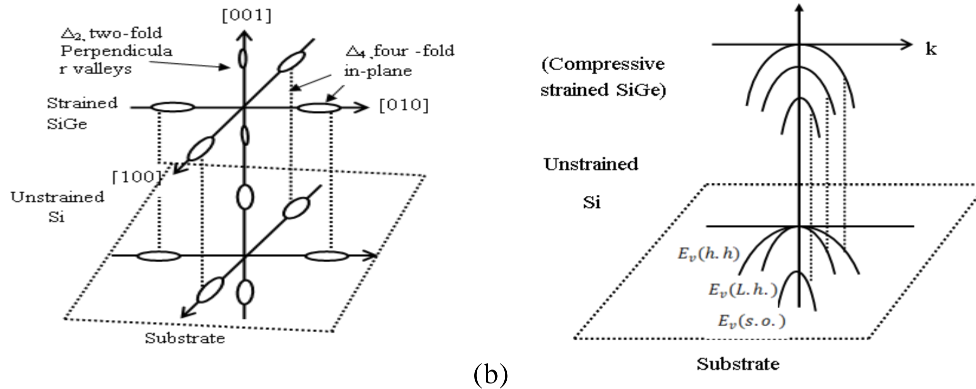

Figure 1. (a) Illustration of the Energy Shift of the Six Δ Valley in Strained SiGe for Growth Along the (001) Axis in Conduction Band [11], (b) Hole Mobility for Compressive Strained SiGe Introduced Si in Base of HBTs [11]

The effective density of states for the valence band decreases when the Ge composition is more. By the effect of uniaxial stress the valence band splits the heavy and light hole bands and change the structure as depicted in Figure 1(b). The coupling interactions of spin-orbit band with heavy and light hole bands can be significant under large strain which was reduce the effective mass has been reported by several authors [12, 13]. Monte Carlo simulation of electron mobility having doped SiGe at room temperature (μ_n) having 50% higher than that for Si due to smaller effective mass [14], in addition to Phonon , impurity and alloy scattered mechanisms , strain has determined carrier mobility. Bufler *et al.*, [15] have reported that minority carrier mobility in unstrained and strained SiGe are different as in the case of Si. In case of coherently

Copyright ⓒ 2014 SERSC

strained layer, the conduction band of the alloy remains undistorted for Ge mole fraction below 30% and only strain-induced energy shift occurs in the conduction band valleys. The shift in energy yields two different mobility values. One perpendicular to the growth plain is having a value larger than the unstrained mobility and the other parallel to the growth direction is having the smaller value [15]. The alloy scattering was limited to mobility components along the direction of perpendicular and parallel to the growth plain for a coherently strained SiGe layer [16]. This analytical mobility models for strained SiGe is found to be comparable to the MC simulation results reported by Bufler *et al.*, [15]. The parallel component of mobility decreases as Ge mole fraction increases. The perpendicular components of the mobility remains almost the same as in the case of 10^{17} cm^{-3} doping due to the dominating alloy scattering at lower doping level . But in case of 10^{18} cm^{-3} doping level or higher, the strain layer shows a higher mobility than Si and the trend continues till 10^{20} cm^{-3}doping level.

In SiGe alloy hole transport model based on the three anisotropy and non-parabolic hole band is much more complicated than for the electron due to complex hole band structure and additional alloy scattering mechanism. Bufler *et al.*, [15], using Monte Carlo simulation, have calculated the majority and minority drift motilities for holes in unstrained and strained SiGe up to a Ge content of 30% and a doping concentration up to 10^{20} cm^{-3}. The doping dependence of hole mobility of strained SiGe for a low Ge content ($x<0.2$), the computed mobility has excellent result [17]. The relation to the mobility of the electric field which as proposed by Caughey and Thomas and further modified by Thornber [18]. Bufler *et al.*, [15] have reported that the Ge mole fraction dependence of electron and hole saturation velocity, the recombination processes in bulk Si and strained SiGe are taken Shockley–Read–Hall (SRH) and Auger recombination. This types of recombination involved excitons and Shallow –Level traps at a low temp. In SRH recombination is occurs at low doping concentrations and Auger recombination is more suitable for narrow band gap semiconductors [11].

4. Device Structures and Simulation

Two-dimensional device simulations are done for the strained SiGe HBT structure and Si BJT structure by using the Silvaco Atlas device simulator [19]. As shown in Figure 2. A strained $Si_{0.88}Ge_{0.12}$ base of 100 nm is used. The emitter and the collector are made of silicon. And the emitter and the base width are approximately 0.1 µm each, which has followed by 0.6 µm of n^- collector. The mole fraction in the emitter-base transition region changes from its initial value $x = 0.03$ to its final value $x = 0.12$ inside the base over a distance of 250 Å. The base-collector transition region starts at the p-n junction and extends 300 Å into the collector. The value $x = 0.12$ was chosen based on the desired base width of 0.1 µm, which determines the upper limit of mole fraction of Ge due to the smaller critical thickness for commensurate growth at higher mole fractions. Device simulation was performed by ATLAS simulator. For Ic-V_{BE} characteristic V_{BE} was varying from 0 to 1V in each case. These two devices were simulated with the same condition to compare and observe electrical characteristics between them.

 Copyright ⓒ 2014 SERSC

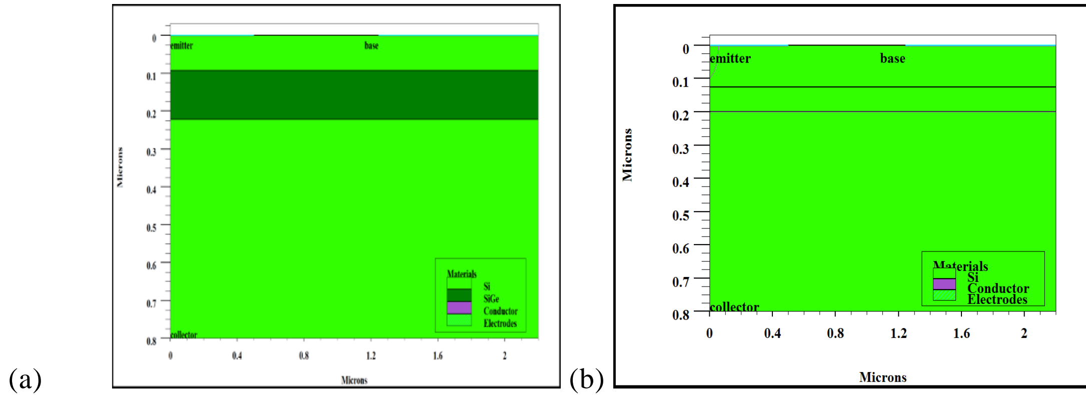

Figure 2. (a)Strained $Si_{0.88}Ge_{0.12}$ HBT (b) Simulated Si BJT for 100nm base Width

5. Device Structures and Simulation

Drift-diffusion model for SiGe-HBTs, based on the BJT modeling, is used in the simulation. The model equations account for valence band discontinuity, heavy doping effects and high collector current effects. The doping profile along the center of the emitter, as estimated using the built-in functions of the program is shown in Figure 3(a).

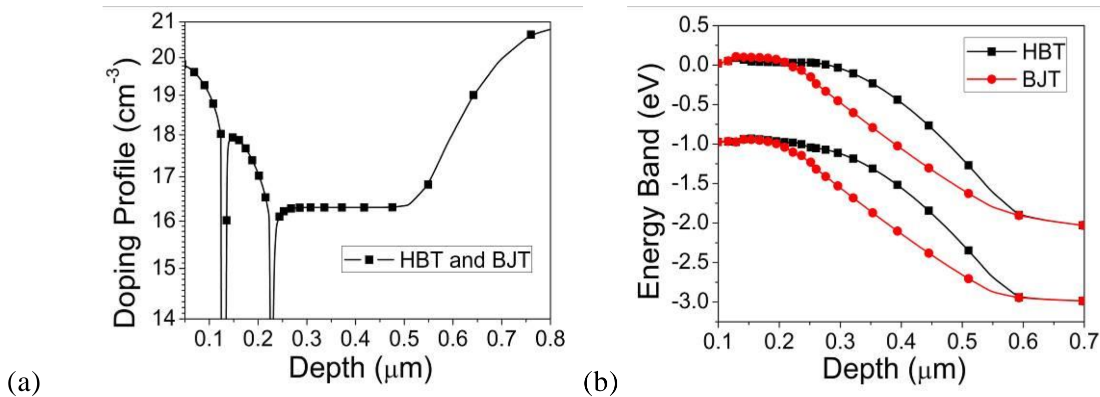

Figure 3. (a) Net Doping Profile Across the Middle of the Emitter,(b) Energy Band Gap Variation for Si and SiGe Devices (Along the Center Line going from the Emitter to the Collector Contact)

The Ge mole-fraction varies linearly from 2% at the emitter-base junction to 12% at the base-collector junction. Here it is shown that small amounts of boron diffused out from the heavily doped SiGe base into more lightly doped emitter and collector regions can seriously degrade the collector current enhancement by forming parasitic potential barriers for electrons in the conduction band at Si/SiGe interfaces. It is important to guard against the presence of such barriers. It is therefore, useful to examine the energy band diagrams for the HBT to reveal the existence of parasitic barriers when the junctions are not formed in SiGe. A band diagram is shown in Figure 3(b). For applied voltages of V_{BE}=0.7 and V_{CE}=2.0V.Apparently there are no parasitic barriers.

Copyright ⓒ 2014 SERSC

The cross-section of this device possesses a 100μm thick Boron-doped strained-SiGe base layer with a peak base doping of 5×10^{15} cm^{-3} and Emitter doping of 8×10^{20} cm^{-3} also collector doping of 2×10^{16} $cm^{-3.}$ Figure 4. shows the vertical profiles of electron density and mean electron drift velocity obtained from HBT and BJT, in steady state for V_{BE}=0.7V and V_{CE}=2.0V, respectively. The peak electron charge in the base/collector region obtained from HBT is compared with BJT.

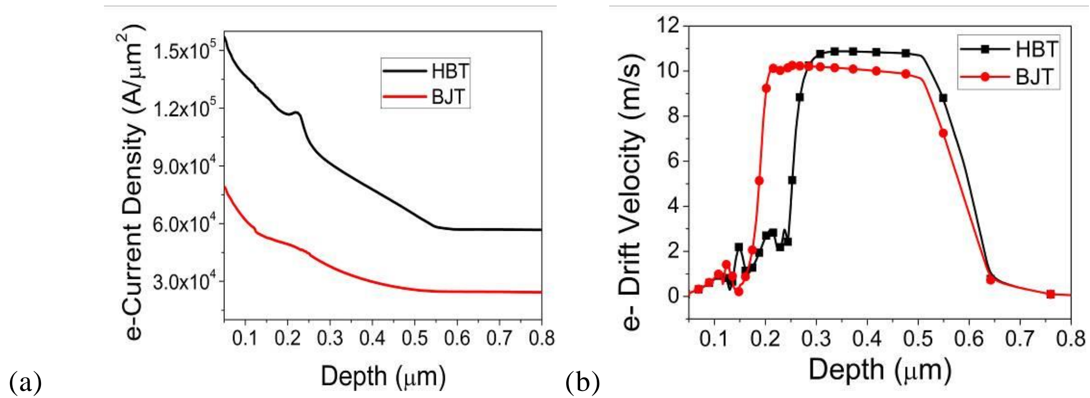

Figure 4. (a) Vertical Electron Density Profiles of Si BJT& SiGe HBT at V_{BE}=0.7 V and V_{CE}=2.0V, (b) Electron Velocity Profiles in the Base (100nm) of the SiGe-HBT Obtained by the DD Simulation at V_{BE}=0.7V and V_{CE}=2.0V

In Figure 4(b). a velocity overshoot is observed near the base-collector junction. Monte Carlo simulation in heavily doped SiGe at room temperature indicates that the electron mobility is almost 50% higher than that for Si due to smaller effective mass [14]. In Figure 5(a) shows that the mobility of hole of SiGe HBTs is 2 times higher than Si BJT. The Figure 5(b) shows the Electron mobility of Si/SiGe HBTs which is three times higher than BJT.

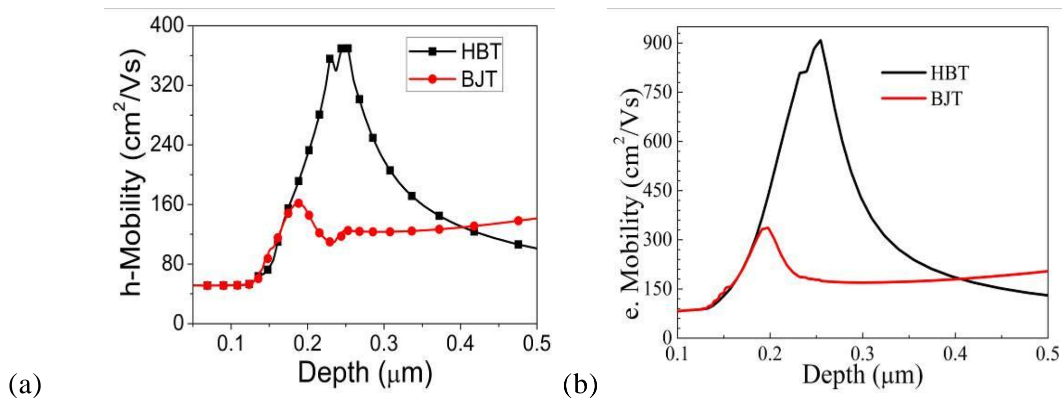

Figure 5. (a)Vertical Hole Mobility of Si BJT& SiGe HBT at V_{BE}=0.7 V and V_{CE}=2.0V, (b) Vertical Electron Mobility of Si BJT& SiGe HBT at V_{BE}=0.7 V and V_{CE}=2.0V

Next, the simulated collector and base current characteristics are presented in Figure 6(a) as a function of base-emitter voltage. The base currents do not show any significant differences, but to obtain the small differences in collector current, the Si

 Copyright ⓒ 2014 SERSC

BJT requires 0.07 V more than the emitter-base voltage. This reduction in turn-on voltage is caused by a decrease in the barrier height for injection of electrons. It is possible to reduce the power dissipation in the circuit environment. On the other hand, due to the smaller band gap in the base, the high temperature range is going to be more restricted than in Si. The mobility is computed using Bufler *et al.*, [15] data. They have reported that minority carrier mobility in unstrained and strained $Si_{0.88}Ge_{0.12}$ are different as in the case of Si BJT.

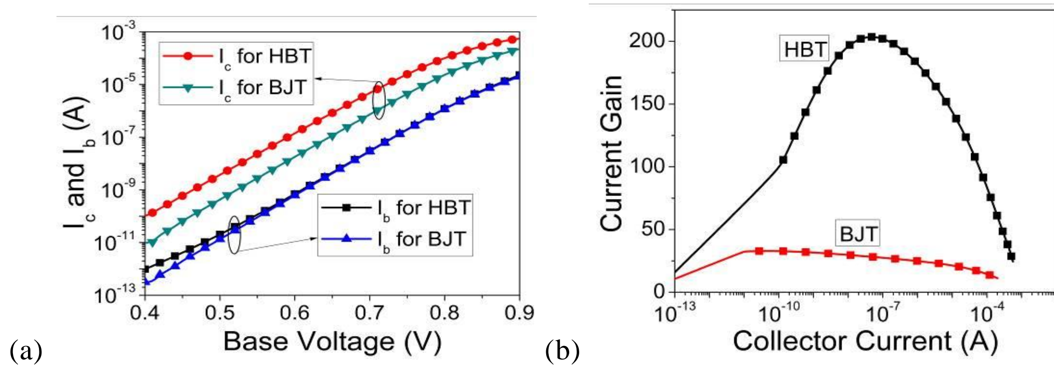

Figure 6. (a)Gummel Plots for the Si BJT and SiGe (graded based) HBT at V_{CE}=2V, (b) A comparison of dc current gain of a Si-BJT and a Trapezoid-Base SiGe-HBT at V_{CE}=2V

The simulated device characteristics for the HBTs and BJT structure (which is shown in Figure 1(a), with a base thickness of 100nm), are shown in Figure 5(a). Here HBTs collector current increases ten times more than the collector current of BJT which is due to the band gap narrowing effect. But current gain comparing SiGe-HBT with trapezoid Ge profile and Si transistors is shown in Figure 6(b). As it can be seen in Figure 6(b), the Ge profile produces the seven fold increment in β for 12% Ge at 300K, since the enhancement depends exponentially on the band gap reduction at the emitter-base junction. In the conventional Si-BJT, β is inversely proportional to the integrated base charge. Since base doping cannot be increased indefinitely while maintaining adequate β. This Ge profile is particularly useful in realizing a transistor with either a very high β,or a moderate β with lower intrinsic base resistance[20].

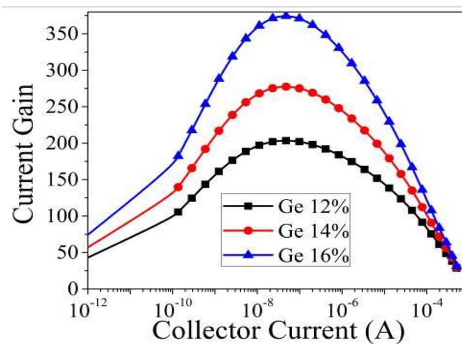

Figure 7. DC Current Gain of SiGe HBT Vs Collector Current with Different Ge Mole Fraction

Copyright ⓒ 2014 SERSC

By using the different Ge mole fraction, from the current gain Vs collector current curve as it can be seen in Figure 7 that the gain gradually increases two times when the Ge percentage increases 2% more.

6. Conclusion

In this paper, we described a 100nm Si/SiGe HBTs designed for high gain and lower turn on voltage operation. We have shown this by using the device simulator that the low field electron mobility in strained SiGe layers to enhance the performance of bulk mobility with doping levels $N_D>10^{15}$ and $x<0.2$ it exceeds the Si mobility. In both cases we calculated a substantial improvement in current gain that is seven fold increases in β for 12% Ge at 300 K. Because of the reduced band gap in the base, the $Si_{0.88}Ge_{0.12}$ device also exhibits a reduction in turn-on voltage of 0.7V, which helps reduce power dissipation and increase electron density, electron drift velocity in base/collector region. Gummel plots have been generated for a Si BJT and a $Si_{0.88}Ge_{0.12}$ HBT for different values of Ge mole-fractions in the base. This article has mainly focused on the performance enhancement by strained Si/SiGe HBTs Technology.

References

[1] B. Senapati, C. K. Maiti and N. B. Chakrabati, "Silicon Heterostructure Devices for RF Wireless Communication", Int'l.Conf. on VLSI Design, Calcutta, **(2000)**, pp. 488-491.
[2] SC Jain, Germanium-Silicon Strained Layers and Heterostructures, Academic Press Inc, New York, **(1994)**.
[3] C K Maiti and G A Armstrong,Editors Application of Silicon-Germanium Heterostructure Devices Inst of Physics Pub, UK, **(2001)**.
[4] N Zerounian, F Aniel, R Adde & A Gruhle Electronics Lett. 36, 1076 **(2000)**.
[5] B Pejcinovic, L E Kay, T W Tang and D H Navon, IEEE Trans Electron Dev. 36, 2129 **(1989)**.
[6] N.King and A. Victor, IBM MicmNews.5, 5 **(1999)**.
[7] B.Senapati and C. K Maiti,IEEE ICPWC. 9**(2000)**.
[8] S.M. Sze ,Kwok K.Ng Physics of Semiconductor Devices,John Wiley & Sons, U.K.**(2007)**.
[9] D B M Klaassem, J M Slotboom and H C Degraff , Solid State Electron 35, 125 **(1992)**.
[10] P.I Rockett,IEEE Trans. Electron Devices 35, 1573 **(1988)**.
[11] B Senapati, IETE Journal of Research 53, 215 **(2007)**.
[12] M V Fischetti & S E Laux, J. Appl Phys. 88, 2234 **(1996)**.
[13] T Manku & A Nathan, J. Appl Phys. 69, 8414 **(1991)**.
[14] L E Key and T W Tang, Monte Carlo , J. Appl Phys. 70, 1483 **(1991)**.
[15] F M Bufler , P Graf , D Meinerzhagen, D Adeline,M M Rieger,H Kabdel and G Fischer, IEEE Electron Device Lett. 18, 264 **(1997)**.
[16] T Manku and A Nathan , IEEE Trans. Electron Dev. 39 , 2082**(1992)**.
[17] FM Bufler, P Graf and B Meinerzhagen, in Hole transport investigation in unstrained and strained SiGe, J Vac Sc Technol B, **(1998)**,vol. 16,pp 1667- 1669.
[18] K K Thornber, IEEE Electron Device Lett. 3,69 **(1982)**.
[19] ATLAS User's Manual Device Simulation Software, Silvaco International, Santa Clara, Calif, USA, **(2004)**.
[20] Katsuya Oda, Eiji Ohue, Masamichi Tanabe, Hiromi Shimamoto Takahiro Onai, and Katsuyoshi Washio,"130-GHz f_T SiGe HBT Technology",IEEE Electron Devices Meeting,IEDM pp791-794, **(1997)**.

 Copyright ⓒ 2014 SERSC